Evaluation of the Event Detection Level of the Cuban Seismic Network

Eduardo R. Diez Zaldivar[1], Enrico Priolo[*2], Denis Sandron[2], Viana Poveda Brossard[1], Marco Cattaneo[3], Simone Marzorati[3], and Raúl Palau Clares[1]

Abstract

The detection level of a seismic network is a measure of its effective ability to record small earthquakes in a given area. It can vary in both space and time and depends on several factors such as meteorological conditions, anthropic noise, local soil conditions—all factors that affect the seismic noise level—as well as the quality and operating condition of the instruments. The ability to estimate the level of detection is of tremendous importance both in the design of a new network and in determining whether a given network can recognize seismicity consistently or needs to be improved in some of its parts. In this article, we determine the detection level of the Cuban seismic network using the empirically estimated seismic noise spectral level at each station site and some theoretical relationships to predict the signal amplitude of a seismic event at individual stations. The minimum local detectable magnitude thus depends on some network parameters such as the signal-to-noise ratio and the number of stations used in the calculation. We also demonstrate the effectiveness of our predictions by comparing the estimated detection level with those empirically determined from one year of data (i.e., the year 2020) of the Cuban seismic catalog. Our analysis shows, on the one hand, in which areas the current Cuban network should be improved, also depending on the regional pattern of faults, and, on the other hand, indicates the magnitude threshold that can be assumed homogeneously for the catalog of Cuban earthquakes in 2020. Because the adopted method can use current measurements of the seismic noise level (e.g., daily), the proposed analysis can also be configured for continuous monitoring of network state quality.

Cite this article as Diez Zaldivar, E. R., E. Priolo, D. Sandron, V. Poveda Brossard, M. Cattaneo, S. Marzorati, and R. Palau Clares (2022). Evaluation of the Event Detection Level of the Cuban Seismic Network, *Seismol. Res. Lett.* **93**, 2048–2062, doi: 10.1785/0220220016.

Supplemental Material

Introduction

Estimating the detection capability of a seismic network is of tremendous importance both to design a new network and, for an existing network, to evaluate its performance and define how to improve it. Some of the possible motivations of implementing and performing such a task are: consistent and uniform recognition of the seismicity over the whole target area of monitoring, evaluation of the network setup and possible changes to it to achieve a target magnitude of completeness in the resulting earthquake catalog, continuous control of the network operativity and efficiency through the measurement of the acquired data, and its overall performance.

The detection capability can be expressed in some different ways. One of them is the magnitude of completeness, which is defined as the lowest magnitude of events that a network is able to record reliably and completely (Schorlemmer and Woessner, 2008). This concept has also been formulated by a probability approach by Nanjo *et al.* (2010). An alternative way is that of estimating the minimum magnitude of earthquakes that can be detected or localized over the target area (e.g., Raymer and Leslie, 2011).

Obviously, when evaluating the detection capability, spatial and temporal errors in event location implicitly play a relevant role and should be assessed independently, to improve the overall estimation of the seismic network performance (Zivčić and Ravnik, 2002; D'Alessandro *et al.*, 2011).

There also are some different and not less important points of view in evaluating the performance of a network, for example, that of measuring the amount of time needed to detect an earthquake, an issue that is of primary interest for early-warning systems (e.g., McNamara *et al.*, 2016) or that of continuously assessing the quality of the monitoring, as described by

1. Centro Nacional de Investigaciones Sismológicas (CENAIS), Santiago de Cuba, Cuba, https://orcid.org/0000-0002-1323-8451 (ERDZ); https://orcid.org/0000-0003-1971-8592 (VPB); https://orcid.org/0000-0003-3864-2159 (RPC); 2. Istituto Nazionale di Oceanografia e di Geofisica Sperimentale—OGS, Trieste, Italy, https://orcid.org/0000-0002-4392-6781 (EP); https://orcid.org/0000-0002-1143-9954 (DS); 3. Istituto Nazionale di Geofisica e Vulcanologia (INGV), Osservatorio Nazionale Terremoti, Ancona, Italy, https://orcid.org/0000-0001-6017-8861 (MC); https://orcid.org/0000-0002-5803-4882 (SM)

*Corresponding author: epriolo@inogs.it

Petersen *et al.* (2019) for the European Alp Array network. However, those issues are quite far from the interest of this study.

An important concept is that the detection capability is a property that is neither uniform in space nor constant in time. This is due to several causes, such as, for example, instrument operation, the quality of the overall hardware, which can be different among stations and degrade over time, the atmospheric conditions, the anthropogenic noise, and the local soil conditions. All of these factors affect the noise level of the recorded signal, an amount that can be measured and assessed in the spectral domain with an appropriate processing plan.

The Caribbean region has a documented history of natural catastrophes (i.e., hurricanes, volcanoes, earthquakes, and tsunamis) with a high economic cost and human lives losses. The last 500 yr of documented history highlight several relevant earthquakes and associated tsunamis, such as the events that occurred in Jamaica in 1692, the Virgin Islands in 1867, Puerto Rico in 1918, Cuba in 1932 and 1992, and the Dominican Republic in 1946. Haiti was the area most affected by earthquakes in this century, with the M_w 7.7 event of 28 January 2020—the largest earthquake recorded in the area since the instrumental age began—and another three moderate-to-strong events (i.e., the M_w 7.0 in 2010, M_w 5.9 in 2018, and M_w 7.2 in 2021, respectively).

The location of the Cuban island right in the middle of the Caribbean Sea is strategic for improving the overall seismic monitoring capabilities in the Caribbean region. As part of regional cooperation, the Cuban Seismological Service offers the data of 19 broadband stations installed in the country and more than 40 accelerographs operating in the southeastern part of Cuba through the service provided by Incorporated Research Institutions for Seismology (IRIS, 2017) and International Federation of Digital Seismograph Networks. Thus, assessing the performance of such a monitoring system, as is already done for other networks in the Caribbean area, may contribute to strengthening the overall monitoring system and homogenizing the contributions provided by every single network. In this respect, we mention, among others, the studies performed by Clinton *et al.* (2006) with the analysis of the seismic monitoring in Puerto Rico; McNamara *et al.* (2016), who assessed the performance of the seismic networks installed in the Caribbean region; and De Zeeuw-van Dalfsen and Sleeman (2018), who presented the results of seismic and volcanological monitoring network in the Dutch Antilles.

This article is deeply grounded on the work done by Marzorati and Cattaneo (2016), which developed the software to assess the minimum detectable magnitude of a network and applied it to the Marche–Umbria regions (Italy). However, some other studies are worth being cited for the reader's benefit, as Greig and Ackerley (2014), who developed a tool to assess the network performance by estimating both location accuracy and magnitude of completeness, and apply this technique to a seismic network located in the New Madrid seismic zone (central United States); Franceschina *et al.* (2015), who assessed the detection capability of a new local network realized for monitoring the carbon dioxide (CO_2) geo-sequestration in the depleted gas storage field of Cortemaggiore (Po Plain, northern Italy); Gestermann *et al.* (2016), who investigated the spatiotemporal variation of the completeness magnitude in the northern Germany basin area, an area that hosts several natural gas fields, taking into account the noise levels and geometry of the changing seismic network; McNamara *et al.* (2016), who estimated the minimum detection magnitude (for moment magnitude M_w) and *P*-wave detection time for the Caribbean region.

In this article, we determine the detection level of the Cuban seismic network using the empirically estimated seismic noise spectral level at each station site and some theoretical relationships to predict the signal amplitude of a seismic event at individual stations. We will estimate the distribution of the minimum local detectable magnitude and evaluate the number of triggered stations for a reference magnitude M_L 1.0, which is assumed as a possible future target for the completeness of the Cuban earthquake catalog. We eventually demonstrate the validity of our predictions by comparing the estimated detection level with those empirically determined from one year of data (i.e., the year 2020) of the Cuban seismic catalog.

We think that the analysis and results shown in this article may have a potential interest wider than just the regional scientific one. On the one hand, the implementation of continuous, or at least regular, quality control allows network operators to investigate the characteristics of earthquake catalogs better and, in particular, to avoid attributing possible variability in seismicity rates due to variations in both the seismic network and background seismic noise to active tectonic causes. On the other hand, our procedure can be applied to predict or assess the quality of any seismological network. Let us think in particular of local networks dedicated to monitoring the seismicity of underground industrial activities, for which a level of performance must be guaranteed at the design level and demonstrated later during monitoring operations.

Tectonic environment

Geographically, the Cuba island belongs to the Caribbean region, the area at the west of the northern Atlantic Ocean between North and South America. It is a complex region from a geological and tectonic point of view, for which different and sometimes controversial opinions on its evolution have been formulated over time. Figure 1a shows the position of Cuba in the Caribbean tectonic context.

Initially, some authors claimed that Cuba belongs to the North American tectonic plate and that its southeastern edge borders the Caribbean plate (Mann *et al.*, 1995; Lundgren and Russo, 1996; Mann, 1999). This edge approaches a transcurrent fault system parallel to the coast and featuring left lateral movement, known as the "Oriente" (also called "Bartlett-Caymán") fault system zone. This tectonic structure affects

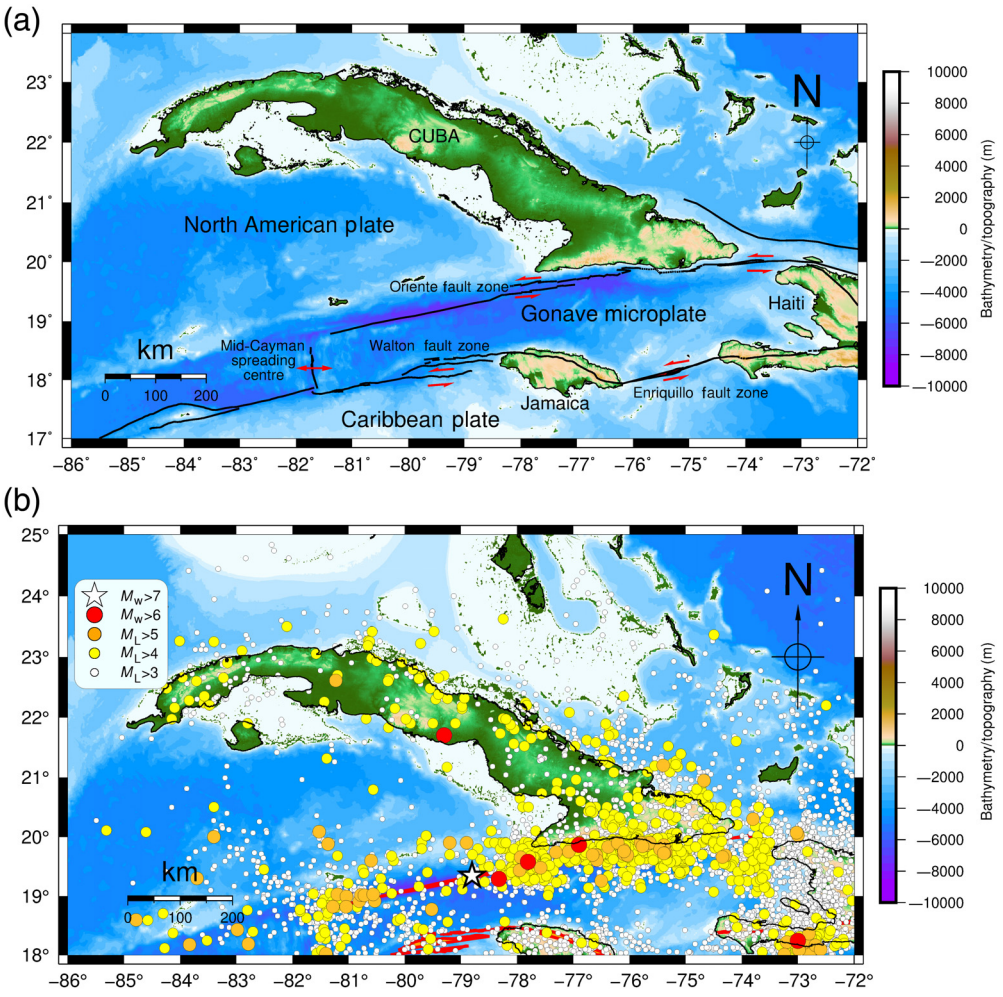

Figure 1. Cuba island in the Caribbean tectonic context. (a) The main fault systems (red lines; red arrows represent the fault relative movement), with the Bartlett-Cayman fault system (Oriente) and other relevant fault systems in the region (Mann *et al.*, 1995; Lundgren and Russo, 1996; Mann, 1999; Mann *et al.*, 2004). (b) Seismicity in Cuba and surrounding areas from 1965 to 2020, taken from the National Centre for Seismological Research (CENAIS) historical general catalog and reprocessed for this study by Arango (2021). The magnitude range from 3 to 7 is considered (see colors in the legend). We used local magnitude M_L for magnitude not exceeding 5, and moment magnitude M_w for stronger events. The color version of this figure is available only in the electronic edition.

not only the territory of Cuba but also other Caribbean islands such as Jamaica, Cayman Islands, Puerto Rico, and Hispaniola.

However, some more recent studies on this plate boundary zone (DeMets, 1990; Deng and Sykes, 1995; Calais and Lépinay, 1989, 1993) have demonstrated, also using arguments based on crustal deformation modeling, the existence of a microplate between the North American and the Caribbean plates, namely the Gonave microplate, previously proposed by Rosencrantz and Mann (1991) (Fig. 1a).

The Gonave microplate is a semirectangular microplate that has an area of approximately 190, 000 km^2 and borders the North American and Caribbean plates to the south and north, respectively (Heubeck and Mann, 1991; Mann *et al.*, 2004). The "Oriente" fault zone is responsible for most of the strong earthquakes that occurred in this area, as inferred from the estimation of energy accumulated by the relative movement between the plates described earlier (Arango, 2009).

Seismicity

Cuba's seismicity features both "interplate" and "intraplate" characters. Interplate seismicity is related to the Oriente fault zone and features a higher frequency of occurrence of earthquakes that can reach large magnitude ($M_w > 7.0$) and depth greater than 20 km.

More than 90% of the earthquakes that strike the country occur in the southeastern area of Cuba (Álvarez and Bune, 1977; Álvarez *et al.*, 1991, 1999; Moreno *et al.*, 2002). However, some moderate seismicity is also associated with minor faults existing inland of Cuba, which produced some moderate earthquakes with considerable damage (Chuy, 1999).

The map in Figure 1b shows the earthquakes recorded in Cuba (magnitudes between 3.0 and 7.0 on the Richter scale) from the appearance of the instrumental record to the present and highlights the overall seismicity, with both interplate and intraplate earthquakes. The historical earthquakes, although not presented in this map, follow the same tendency in terms of location and estimated magnitude (Chuy, 1999).

Besides the large and moderate earthquakes, it is also important to record the weak seismicity accurately, as it is crucial for defining the seismic regime of the area as a whole, as well as for estimating the accumulation or release of tectonic deformation, the scattering, and attenuation properties of the crust, and the seismic hazard, among other quantities (Arango, 2021). The map in Figure 2a shows the recorded earthquakes with M_L between 0.4 and 3.0 during the year 2020.

Seismic network

Historical literature dates the deployment of the first geophysical–seismological instruments in Cuba at the beginning of the

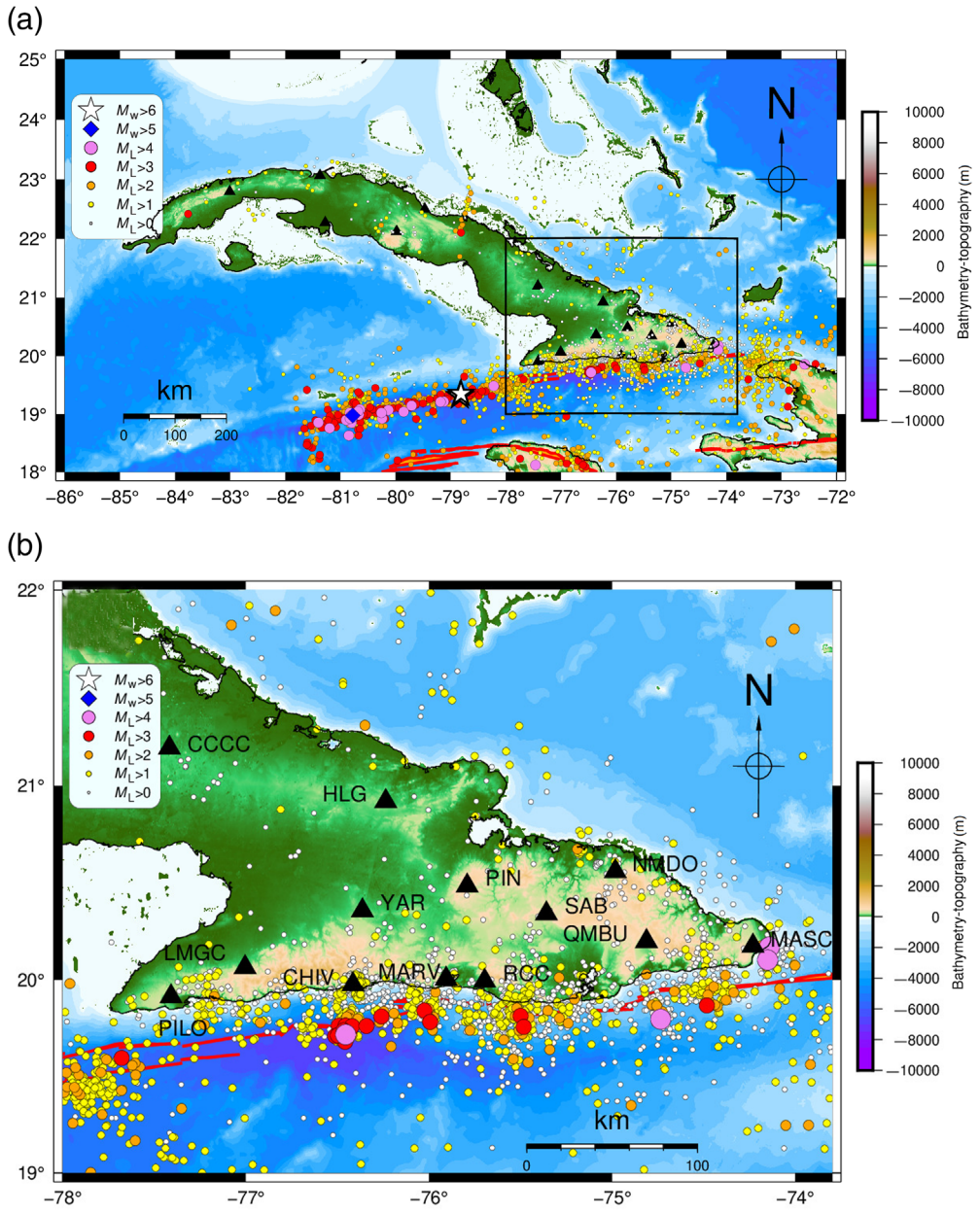

Figure 2. Seismicity of the year 2020 in Cuba and location of the Cuban National Seismological Service stations. (a) Map of the earthquakes in 2020 in Cuba and surrounding areas and the location of seismological stations used in this study (black triangles). The magnitude ranges from 0.4 to 7.7 (see colors in the legend). Other details as in Figure 1. (b) Zoom of the previous map emphasizing the eastern part of Cuba. The color version of this figure is available only in the electronic edition.

twentieth century, with a Bosch–Omori seismometer in Havana city managed by the Jesuit priests. However, the systematic instrumental seismic recording in Cuba began in 1964, with the installation of the first seismological station in Soroa (SOR), in the western part of the country, followed the next year by the second station in Río Carpintero (RCC), in the southeastern part of Cuba near Santiago de Cuba city (Moreno, 2002a). Both stations, initially equipped with short-period instruments, were the basis for the subsequent development of the Cuban seismic survey.

Later, two different stages can be distinguished: the first one, from the mid-1960s to 1997, with the deployment of analog instrumentation mostly equipped with short-period stations and photographic-visual recording (Serrano and Álvarez, 1983); and a second period, from 1998 to the present, characterized by digital instruments, either short-period, broadband, or accelerometric (Diez Zaldívar, 1999).

At present, the National Seismological Service (SSN in Spanish) manages 19 broadband digital stations with national coverage, which transmit data in real time to the Geodynamic Observatory in Santiago de Cuba city. The name of these stations, coordinates, and type of soil on which they are located are shown in Table 1, whereas their location is indicated in the map in Figure 2b (Diez Zaldívar *et al.*, 2014).

The data recorded by the seismic stations are acquired remotely by the SSN Geodynamic Observatory, which hosts the infrastructure designed for the storage and analysis of these signals. The core of the processing system is a central server equipped with the SeisComP3 software (Helmholtz-Centre Potsdam —GFZ German Research Centre for Geosciences and gempa GmbH, 2008), which is in charge of real-time data acquisition, automatic phase picking, and preliminary estimation of the main parameters of recognized earthquakes (e.g., location, depth, and magnitude). Waveform data are archived in miniSEED format (IRIS, 2022). Offline analysis of the data is performed in parallel manually, to increase the accuracy and detect any seismic event that was overlooked by the automatic system. The two approaches

TABLE 1
Cuban Seismic Network Stations Characteristics

Station Name	Network Code	Station Code	Latitude (N)	Longitude (W)	Type of Soil
Chivirico	CW	CHIV	19.9764	76.4151	Volcanic ash forming layers or strata
Caibarién	CW	CAIB	23.0617	81.3708	Limestones stratified in small layers
Camarioca	CW	CAMR	22.4970	79.4709	Sedimentary rocks
Cascorro	CW	CCCC	21.1934	77.4173	Very hard igneous rocks (granite)
Holguín	CW	HLG	20.9200	76.2361	Igneous rocks (streamers)
Jaguey	CW	CJAG	22.2683	81.2763	Massive karst limestones deep caverns
Las Mercedes	CW	LMGC	20.0646	77.0045	Volcanic ash forming extracts
Nuevo Mundo	CW	NMDO	20.5598	77.4173	Igneous rocks (streamers)
Mar Verde	CW	MARV	20.0052	75.9065	Igneous rocks (basalts)
Maisí	CW	MASC	20.1755	74.2312	Sedimentary rock (calcified hard limestones)
Manicaragua	CW	MGV	22.1144	79.9796	Metamorphic rocks weathered soil
Pilón	CW	PILO	19.9140	77.4085	Stratified volcanic rocks
Pinares Mayarí	CW	PIN	20.4855	75.7915	Streamers
Quimbuelo	CW	QMBU	20.1989	74.8127	Compact clusters
Rio Carpintero	CW	RCC	19.9950	75.6965	Very hard igneous rocks
Sabaneta	CW	SAB	20.3418	75.3593	Stratified limestones
Soroa	CW	SOR	22.7932	83.0086	Sedimentary rocks
Yarey	CW	YAR	20.3577	76.3635	Basalt rocks

complement each other and improve the quality of the final result. The data of the earthquakes recognized by the Cuban SSN are gathered in an earthquake catalog in SEISAN format (Ottemoller and Havskov, 2014).

In this article, we use the year 2020 data from the SSN earthquake to validate the results of our analysis (see Data and Resources). This data set is provided as a deliverable of this study in the supplemental material.

Method

This study is focused on determining the detection level of the Cuban network, identifying the number of stations that are capable of recording all earthquakes with a small reference magnitude, considered as the minimum detection threshold to be reached in the future.

Different approaches have been applied in Cuba in the past to assess the detection capability of the Cuban seismic network. Álvarez (2000) proposed the determination of the detection threshold based on the energetic classes analysis. More specifically, they used the Rautián's *Kr* and *Kd* energetic classes, based the first on the measurements of the *P* and *S* waves maximum amplitudes, and the second on the total duration of the earthquake signal, respectively. Gonzales and Arango (1996) used the magnitude per volume wave for the same purpose, whereas Moreno (2002b) proposes a new detection level from the SEISAN digital format catalog using the local magnitude M_L, and assuming that the network is homogeneous and that the attenuation of seismic waves is the same in all directions.

All the previous methods were based on the offline processing of the earthquake catalog. However, as nowadays the data acquisition and processing are almost in real time, some new approaches based on much more massive use of recorded data and empirically measured parameters and allowing a nearly continuous update of the estimations can be implemented.

The approach by Marzorati and Cattaneo (2016) assumes that both the earthquake source and the propagation path can be described theoretically through Brune's spectrum (Brune, 1970) and a suitable spectral attenuation law, respectively, then the seismic noise at each station is the basic observed quantity that can be expressed as a power spectral density (PSD), according to McNamara and Boaz (2005). Because we can calculate theoretically the signal at any station for any given earthquake, the seismic noise level affects directly the observed signal-to-noise ratio (SNR) and influences the detection threshold at each site. Usually, the SNR threshold is set at no less than 2 in seismic network packages, for the frequency band of interest (which depends on the network target).

Two configuration parameters are fundamental for our method to simulate the earthquake detection, as usually carried out by nearly any seismological network software: one is the SNR, whereas the other one is the minimum number of triggered stations for declaring an event. In our simulations, we will test different values for those parameters.

The mean (rms) noise amplitude at each station is calculated independently in the form of a PSD function; this is performed using the PASSCAL Quick Look eXtended (PQLX) program (McNamara and Boaz, 2005).

The method discretizes the study area into a regular 3D mesh, where each node represents a hypothetical earthquake hypocenter with a certain magnitude. We set a grid step of 0.015°. The theoretical amplitude of the earthquake signal is calculated at each node based on the source-station distance through the so-called attenuation law, which can be defined either empirically or theoretically. In this study, we use the empirical attenuation law currently in use at the SSN of Cuba (Moreno, 2002b). Then, the method calculates the SNR for the current value of noise PSD at each station and selects the triggered stations, that is, those stations for which the SNR is larger than the assumed threshold. If the number of triggering stations is more than the assumed threshold number, then the event is declared detected and the node is switched on. Those operations are performed for earthquake magnitudes ranging in a selected interval, thus in the end the method provides the answer (YES or NO) on whether an earthquake with a given magnitude occurring on a given location (i.e., a node of the volume) would have been detected or not by the seismic network with the assumed parameter configuration.

The results are represented graphically as isolines in a map, the so-called detection map. As will be shown later, the obtained maps (or isolines) may not be static, that is they may change over time due to local, anthropic, temperature, cultural noise, and other effects. The result depends on how the seismic noise is calculated and interacts with the recorded signal.

Waveform data set and processing

The geographic area considered in this study is latitude 18°–25° N and longitude 70°–87° W. It corresponds to the effective coverage area of the Cuban network, designed for the detection of the local and regional earthquakes.

In this study, we used both the waveform recordings and the locations performed by the SSN network during the year 2020. To evaluate the network at its current state of development and to the best of its current performance—this means with all the new sensors and the stabilization of the real-time data transmission—we use only the last full year of data, that is, the year 2020. For assessing the seismic network performance, we analyze the continuous waveform data recorded by each station using a statistical approach, as the signals are mainly composed of a stochastic signal. In particular, data are processed by the PQLX, which is an open-source software package distributed by IRIS (2017) for evaluating the performance of the network seismic station and the quality of the recorded data (McNamara and Boaz, 2005, 2010). It calculates the PSDs and the probability density function (PDF) from the full waveform by processing several trace segments having a predefined time length and overlap, respectively. The PSDs are stored in a MySQL database, which allows a specific series of PSD to be accessed through a user interface.

In addition, PQLX allows the estimation of several statistical parameters, as the mode, the mean, and the expected value at different percentiles (e.g., 10, 90, and 95). As will be discussed in the following, the determination of the detection capability of the seismic network relies on the use of these parameters.

In our study, we used temporal windows of one-hour duration and 50% overlap. Waveform data are first corrected for the instrument response (by deconvolution with the instrument response function), then, they are passband filtered in the frequency band 3–15 Hz (0.06–0.33 s), which is the band used for the *S*- and *P*-phase picking for local earthquakes.

Seismic noise in Cuba

Seismic noise studies in Cuba are recent, due to the availability of relatively large amounts of data and suitable analysis tools only in recent times. The most comprehensive study on seismic noise in Cuba is that of Poveda Brossard and Diez Zaldívar (2022), who characterized the seismic noise and its sources for all the stations of the Cuban seismic network.

In general, the Cuban SSN instruments are deployed at the surface and are often affected by high-frequency anthropogenic noise. This can have a negative impact especially in the detection of low-magnitude local earthquakes, for which the analyzed frequency band is 1–20 Hz (i.e., periods 0.05–1 s).

In particular, the PSD curves feature two main influencing factors (Poveda Brossard and Diez Zaldívar, 2022), that is, (1) the noise peaks in the period range 2–20 s due to smaller primary ocean microseism generated in shallow waters in coastal regions together with the secondary ocean microseisms generated by the superposition of ocean waves of equal period traveling in opposite directions (period ranges between 2 and 6 s)—a feature that affects nearly all sites as Cuba is an archipelago and therefore all the sites are near the coast—; and (2) the day–night noise variation in the period range 0.05–1 s due to both the human activity cycle near urbanized areas and the influence of the wind on the vegetation. On the other hand, the analyses corroborate the little influence of the Cuban natural season cycle, which has two seasons per year, namely the rainy and dry season, respectively.

As an example of the cases of extreme noise, Figure 3 shows the PDF curves for the vertical component of the "Cascorro" (CCCC) and "Caibarién" (CAIB) stations, respectively. The red rectangle indicates the period band analyzed in this study.

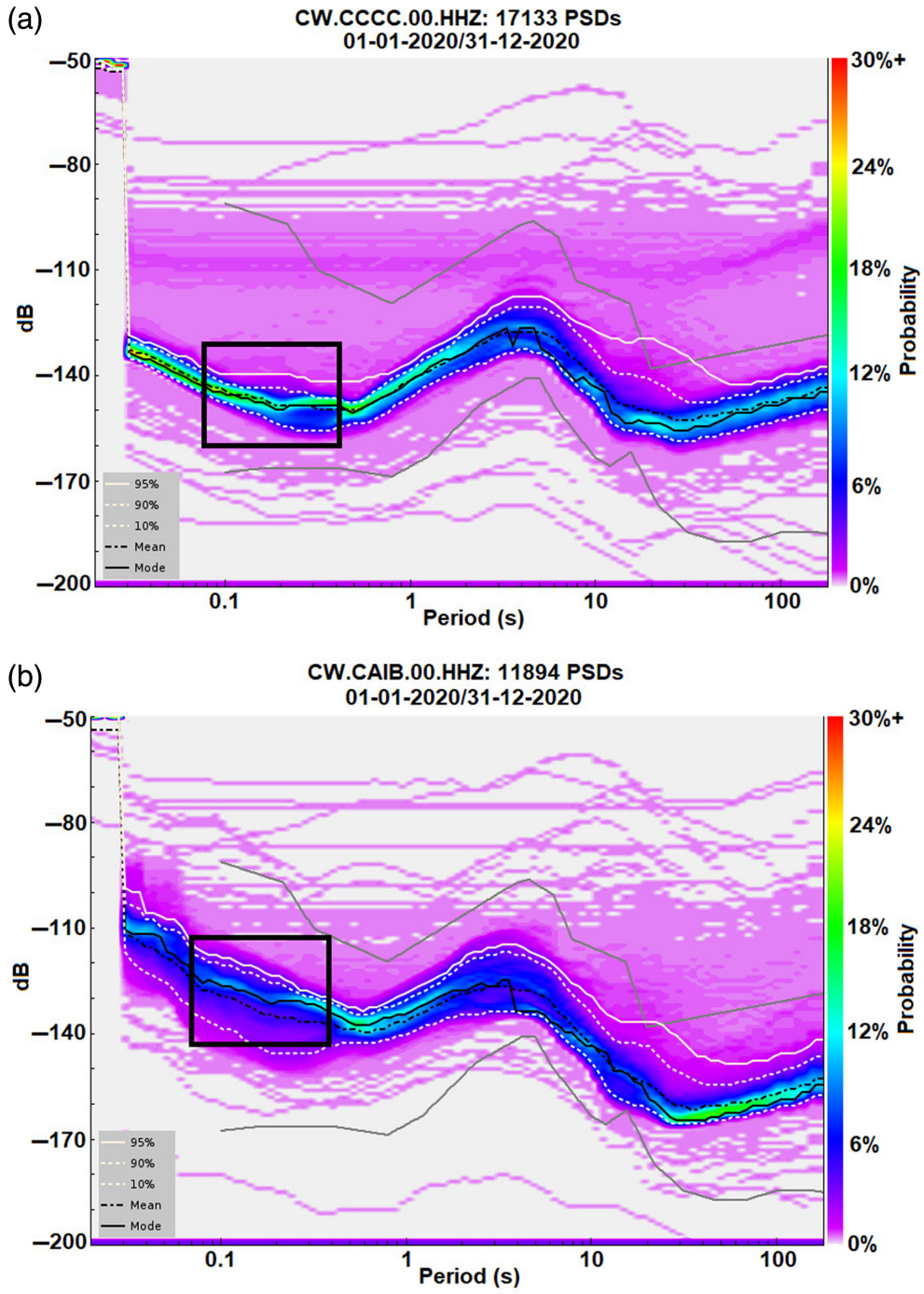

Figure 3. Probability density function plots resulting from the analysis of the continuous seismic noise recording for the two extreme cases of the Cuban network in terms of seismic noise. (a) "Cascorro" station (CCCC), which features the lowest seismic noise level and represents the best case. (b) "Caibarién" station (CAIB), which features the highest seismic noise level and represents the worst case. The black box indicates the band period used in the study. The gray lines represent the reference low-noise and high-noise models (Peterson, 1993). The other lines represent the other estimated statistical parameters, namely the mode (solid black line), the mean (dashed black line), and the expected value at 10, 90, and 95 percentiles (two dashed white lines and solid white line, respectively). The color version of this figure is available only in the electronic edition.

However, all the PSD curves obtained for the Cuban SSN stations are within the range established by Peterson's models (Peterson, 1993); see Figure S1 available in the supplemental material to this article, so it can be concluded that almost all sites have an acceptable noise level according to the current seismology standard.

Estimation of noise amplitude from PSD values

The method by Marzorati and Cattaneo (2016) determines the detection level by comparing the earthquake signal amplitude to the actual noise amplitude through their ratio (i.e., SNR). The noise is provided as an input to the program in terms of a PSD function, which has already been calculated by the PQLX program.

However, as we have to compare the amplitude of the earthquake signal with that of the background noise, we need to convert the PSD into a corresponding waveform amplitude defined in time domain. For doing that, we follow the approach proposed by Aki and Richards (1980) and Bormann and Bergman (2002). If we consider the signal energy concentrated in a limited frequency band $[f_1, f_2]$, the maximum amplitude of a wave $f(t)$ near $t = 0$ can be determined approximately by the product of the so-called energy spectral density with the wave bandwidth, as shown in the following equation:

$$f(t)_{t=0} = |F(\omega)|2(f_2 - f_1), \quad (1)$$

in which $F(\omega)$ is the representation of the arbitrary transient function in the frequency domain $f(t)$ according to Fourier integral transformation.

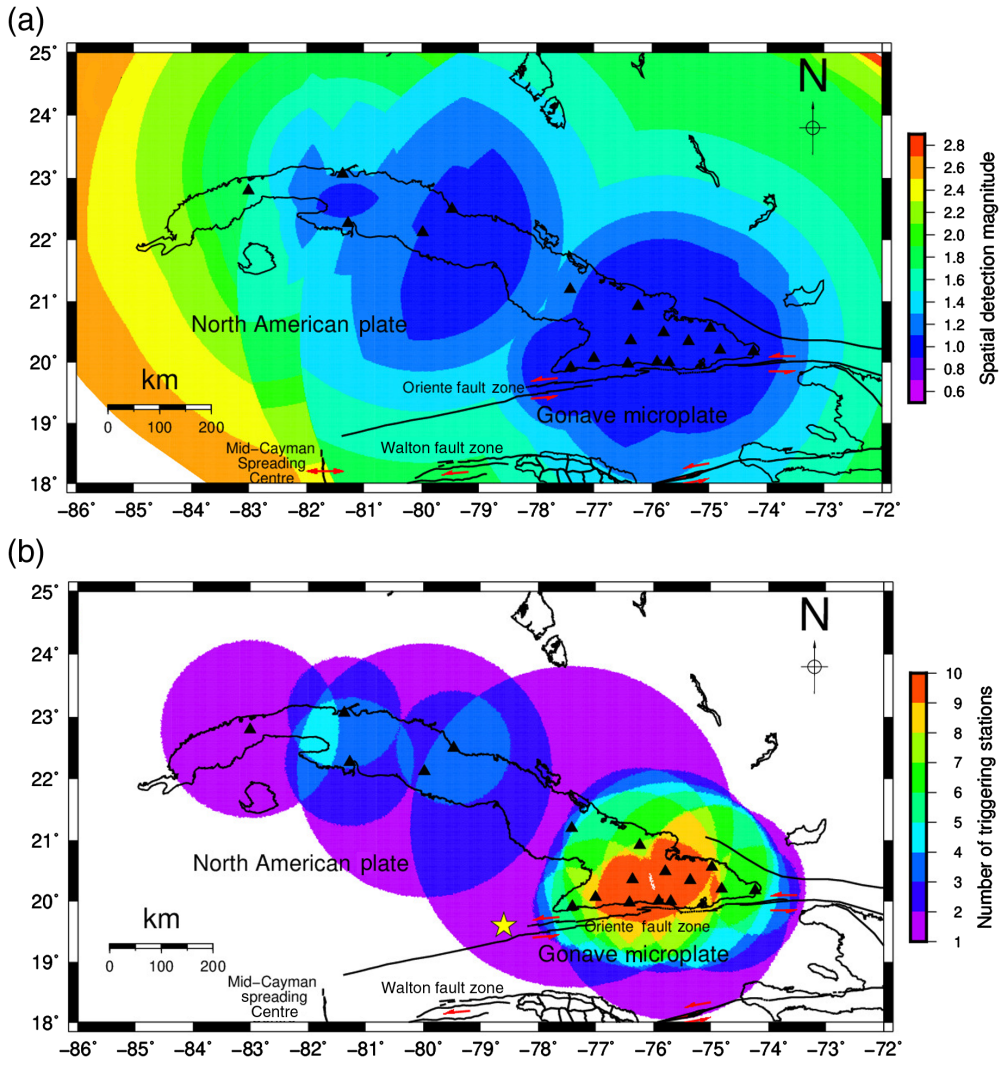

Figure 4. Estimated detection capability of the Cuban seismic network for an average scenario, that is, using the statistical parameter "Mode of the power spectral density (PSD)." A signal-to-noise ratio (SNR)-tolerant condition of SNR = 2 for all stations is assumed. The red triangles represent the seismological stations of the network. The Oriente fault is explicitly shown (black line). (a) The spatial detection magnitude for at least three triggered stations, which corresponds to the minimum number for classical locations. (b) The number of triggering stations for an M_L 1.0 earthquake. The yellow star indicates a weak earthquake occurring offshore the Cabo Cruz area referenced in Results and Discussions. The color version of this figure is available only in the electronic edition.

Using the Fourier transformation property (Parseval's theorem), the energy spectral density is expressed as

$$\int_{-\infty}^{\infty} f(t)^2 dt = \int_{-\infty}^{\infty} \frac{|F(\omega)|^2}{2\pi} d\omega = \int_{-\infty}^{\infty} |F(2\pi\nu)|^2 d\nu, \qquad (2)$$

in which we have the total energy of signal $f(t)$ (proportional to the physical energy) on the left side, whereas the integrand on the right side represents the energy spectral density.

On the other hand, as seismic noise is a stationary random signal, instead of a transient signal, and has infinite energy but finite power, it is more appropriate to substitute the concept of power spectral energy with that of PSD, which represents the energy spectral density per unit time. Then, we can write the mean-square amplitude of noise in the time domain as follows:

$$\langle f^2(t) \rangle = 2P(f_2 - f_1), \qquad (3)$$

in which P is the signal power and is obtained by integrating the PSD over the frequency band $[f_1, f_2]$.

The noise amplitude, which is usually written as root mean square (rms) of the signal, is then obtained as

$$A_{\mathrm{rms}} = \sqrt{2P(f_2 - f_1)}. \qquad (4)$$

The A_{rms} value of the previous equation is the actual noise amplitude, which is used to calculate the SNR.

Results and Discussions

We estimate the detection capability of the Cuban seismic record using the approach by Marzorati and Cattaneo (2016). We chose the PSD "Mode" as a statistical parameter representing the noise level observed at each station. This parameter was extracted, for each station, as the average of the whole set of frequency-dependent mode values calculated day-by-day for the year 2020.

We set at 2 the minimum SNR value for an event that can be detected. Moreover, to comply with the SeisComP3 setting for automatic earthquake detection, we set that at least three stations have to be triggered (i.e., their SNR must be greater than 2) to declare an event as a possible earthquake candidate.

In Figure 4, we show the results of two scenarios. In the first one, we assess the overall detection capability of the network in a very favorable condition, that is, a tolerant SNR threshold of SNR = 2 and event declaration for a minimum of three triggered stations. In the second scenario, we assume a target magnitude of M_L 1.0 for the Cuban grid and calculate, for each grid point, how many stations would be able to detect such an earthquake occurring at that point.

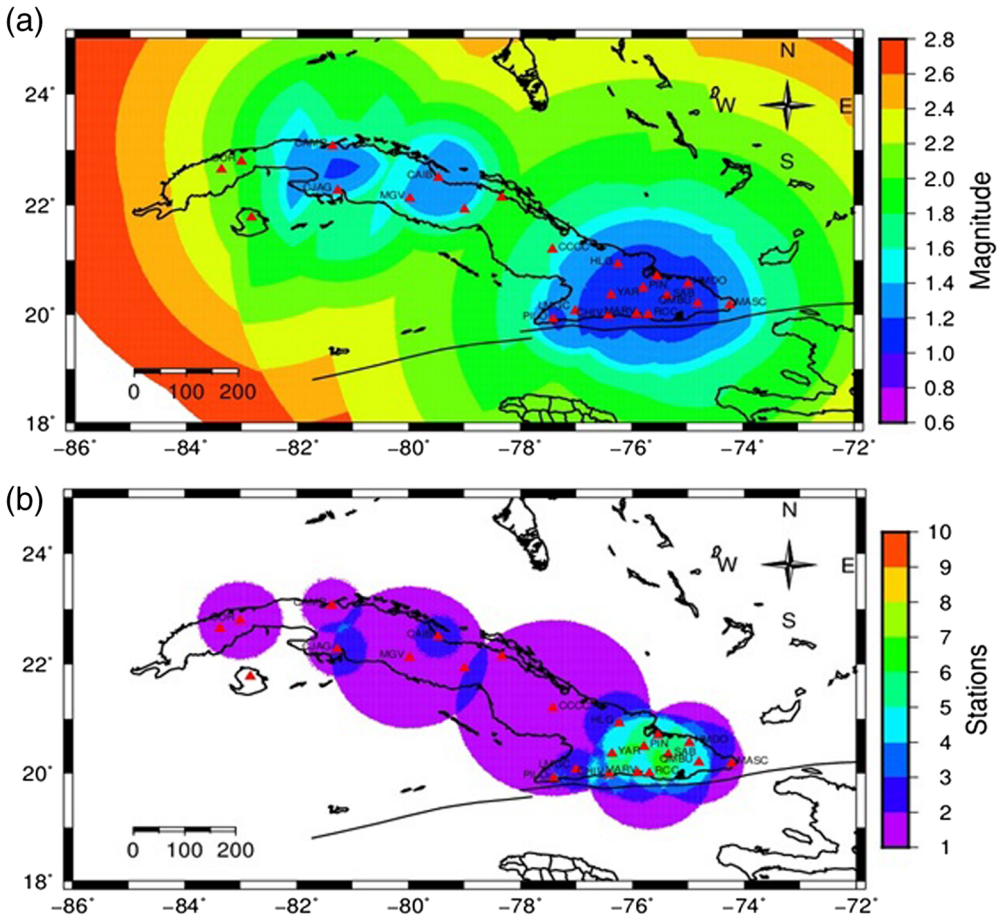

Figure 5. Estimated detection capability of the Cuba seismic network in the worst-case statistical scenario, that is, using the statistical variable "95% of the PSD." An SNR-tolerant condition of SNR = 2 for all stations is assumed. (a) The spatial detection magnitude for at least three triggered stations, which corresponds to the minimum number for classical locations. (b) The number of triggering stations for an M_L 1.0 earthquake. Other details as in Figure 4. The color version of this figure is available only in the electronic edition.

It can be seen that for the eastern part of the country, the network should be able to detect earthquakes with a minimum magnitude M_L 1.0 (Fig. 4a). This is a suitable value for both real-time seismic monitoring and detection of the overall seismicity, respectively, which are the objectives for which the network was designed. The situation worsens significantly in the central-western part of the island, where there are much fewer stations, and those stations are often deployed in noisy sites. In those areas, the minimum magnitude of detection rises from M_L 1.2 to even M_L 2.5 in the extreme part to the west. In practice, $M_L \approx 2.0$ is the minimum detectable magnitude for accurately localized earthquakes (i.e., determined by at least three stations) occurring over 90% of the Cuban territory.

This minimum level of detection is mainly influenced either by the poor quality of some station sites or the installed instruments. Among the latter, we mean sensors deployed on the ground surface and lacking thermal and/or electrostatic insulation, a solution particularly sensitive to natural or anthropogenic noise. A fairly high level of noise along with the occurrence of spurious signals also affects some of the stations recently installed to densify the network (Poveda Brossard and Diez Zaldívar, 2021).

Figure 4b shows the total number of stations that would detect a weak (i.e., M_L 1.0) earthquake. Although in the eastern part of the island, where the Cuban network is dense, a weak earthquake would be detected by 6–10 stations, in the rest of the country, from the middle to the extreme west of the island but a small area, an M_L 1.0 earthquake would hardly be detected by at least three stations, and it would even be outside the coverage range of the network. However, even some parts of the eastern part of the island suffer from poor coverage. For example, a weak earthquake occurring offshore the Cabo Cruz area (i.e., around latitude 20° N and longitude 78°–79 W; see Fig. 4b) would be detected only by few stations (e.g., PILO and LMGC), and this would negatively affect the location quality.

To assess the overall detection capability of the network, we assume a bad condition characterized by a high level of seismic noise, a situation that occurs, for example, during atmospheric disturbances or hurricanes that cause strong winds and ocean waves. To simulate this behavior, we use the statistical parameter "95% of the PSD" in our calculation; other parameters, such as the SNR, are maintained the same. The results are shown in Figure 5.

Figure 5a shows that under bad noise conditions the area where the target magnitude M_L 1.0 is detected reduces considerably: although the eastern part of Cuba still meets this condition, in the rest of the territory, the minimum detected magnitude rises to 1.5 in a large area and reaches 2.4 in the westernmost part of the island. If we focus on the eastern part of Cuba, i.e., where the network features its maximum performance, we note that the central part of the region satisfies the target homogeneously, instead the minimum detected

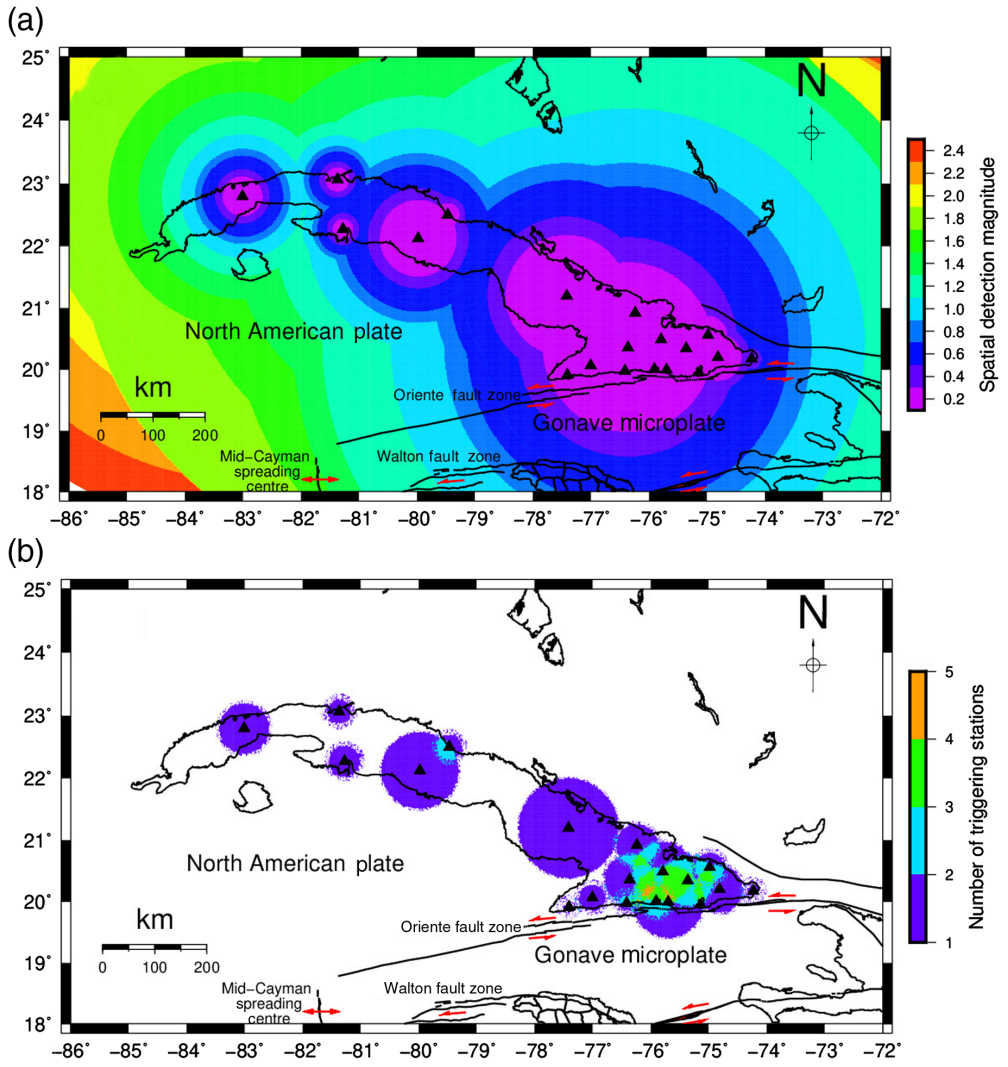

Figure 6. Estimated detection capability of the Cuba seismic network for the limit-case scenarios of further manual inspection. These scenarios represent the maximum expected performance for weak earthquakes. The maps represent the average statistical scenario obtained using the statistical variable "mode of the PSD," and an SNR-tolerant condition of SNR = 2 for all stations, respectively. (a) The spatial detection magnitude for at least one triggered station. (b) The number of triggering stations for an M_L 0.2 earthquake. Other details as in Figure 4. The color version of this figure is available only in the electronic edition.

magnitude worsens to M_L 1.3–1.4 toward the two extreme tips to west (in the Cabo Cruz–Pilon area) and east (in the neighborhood of the MASC station), respectively. The eastern area of Cuba is of particular interest for detecting earthquakes occurring in Haiti, the Dominican Republic, and in the ocean channel (named "Paso de los Vientos") between the islands of Cuba and Haiti, respectively.

On the other hand, Figure 5b shows that under bad noise conditions the target magnitude M_L 1.0 would trigger only one station in a large part of the country and only the eastern part of Cuba would detect an M_L 1.0 earthquake by three triggered stations.

In conclusion, the estimated performance shows that the Cuban seismic network meets the minimum request of being able to localize the seismicity in the most seismic area near the island, that is, the Oriente fault system, whereas it is insufficient to detect and localize with adequate accuracy the low-level seismicity that occurs throughout the archipelago (see Fig. 1a).

Earthquakes detected by one station

About one-third of the earthquakes recorded annually in Cuba and reported in the SSN earthquake catalog are recorded by only one station and are detected through the manual analysis carried out by seismologists. Many of those earthquakes have magnitude $M_L < 1.0$ and are relevant for studying weak seismicity. For this reason, we assess the detection capability of the Cuban network based on single-station triggers. The results are presented in Figure 6, in terms of minimum detected magnitude (panel a) and number of triggered stations for a magnitude M_L 0.2 earthquake (panel b), respectively. Looking at both maps together, it is evident that small earthquakes (i.e., down to M_L 0.2) can be detected in the whole southeastern part of Cuba; however, they will be localized accurately only in a small region (area colored in sky blue, green, or orange), whereas in the rest of the island they will be detected mainly by one single station. For about two-thirds of the national territory, it is impossible to detect earthquakes below M_L 1.0 using automatic analysis tools, a condition that limits heavily any study of intraplate low-energy seismicity.

The main way to improve the detection performance of the network is to increase the number of stations in the western part of the island in the future and choose suitable sites; however, some other actions can help improve the quality of the existing stations, such as deploying posthole or borehole

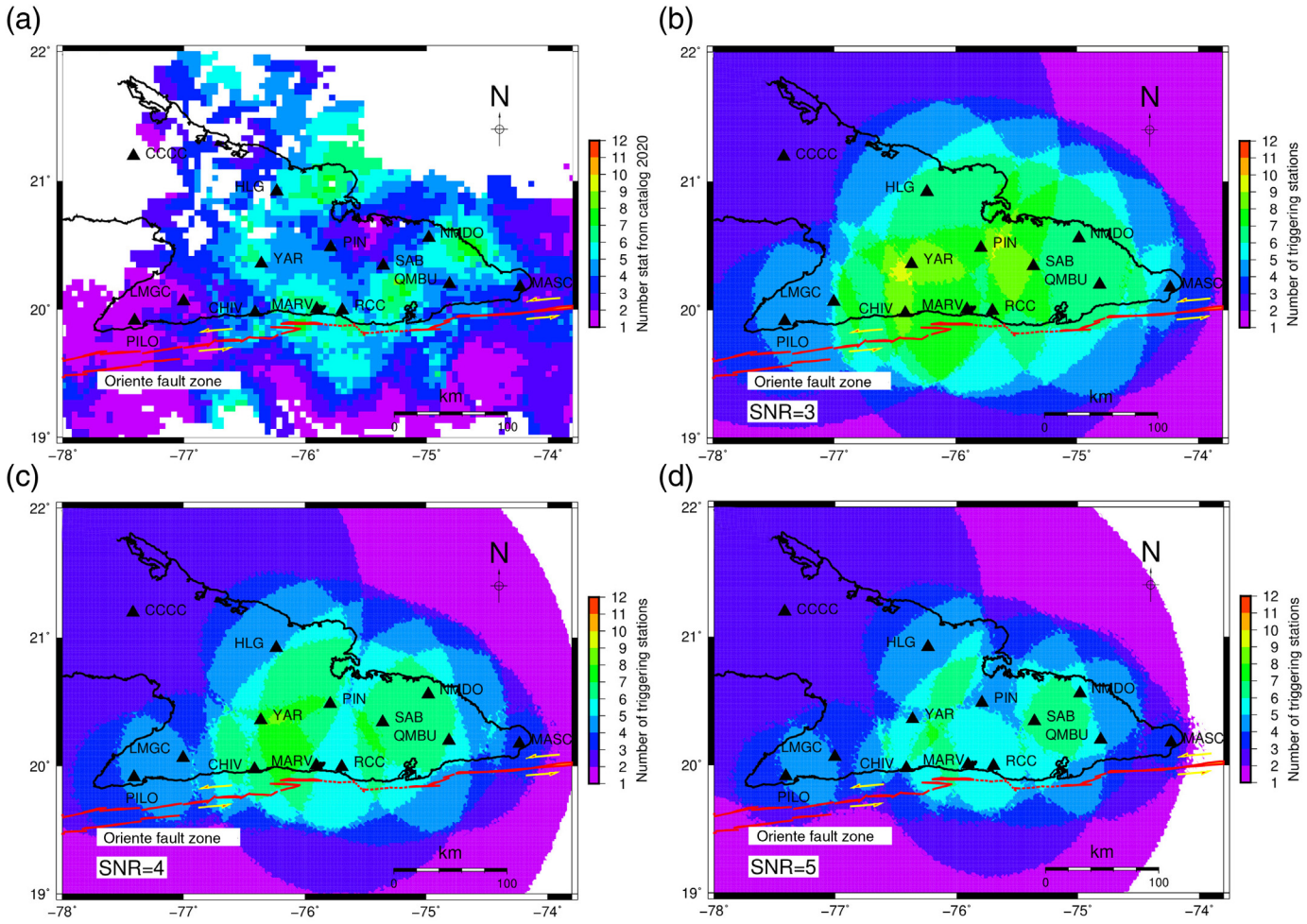

Figure 7. Comparison between the theoretical estimations calculated in this study and the experimental data from the CENAIS 2020 earthquake catalog. (a) Number of stations triggered by an earthquake with a magnitude M_L in the range 0.9–1.1, as inferred from the CENAIS 2020 earthquake catalog. The black dots represent the epicenters of the earthquake catalog. (b–d) Estimated number of stations triggered by an M_L 1.0 earthquake for different SNR values. (b) SNR = 3. (c) SNR = 4. (d) SNR = 5. Other details as in Figure 4. The color version of this figure is available only in the electronic edition.

seismometers and ensuring adequate thermal and electromagnetic isolation of the seismometer.

Validation

To validate our study, we compare the results of our predictions with data from the earthquake catalog. We focus on the number of triggered stations in the case of small earthquakes, that is, earthquakes with M_L near 1.0, which is assumed as a target of completeness for our network. We also restrict this analysis to the eastern part of Cuba because the higher concentration of earthquakes around the Oriente fault zone results in a larger volume of observed data. To get comparable results, we applied the following selection criteria for building the data sets: for the theoretical estimations, SNR = 2 and a minimum of three triggered stations minimum to declare an event; for the observed data, we extracted from the 2020 seismic catalog (CENAIS, 2020) earthquakes with M_L between 0.9 and 1.1 and, for these earthquakes, the number of triggered stations. In Figure A1, we show both the map of the whole 2020 catalog and that of the events with $0.9 \le M_L \le 1.1$ localized in the eastern part of the island (panels a and b, respectively). For each event, the color corresponds to the number of triggered stations.

The maps of Figure 7 compare the number of triggered stations assessed from the observed data (panel a) with those estimated theoretically (panels b–d). For the observed data, the map was obtained through spatial interpolation using the "near-neighbor" algorithm of the Generic Mapping Tools (GMT) software package (Wessel *et al.*, 2013). This algorithm assigns to each node of the grid the weighted average of the values of the nearest data belonging to a circular neighborhood with radius R. The map of Figure 7a was obtained by setting R = 50 km and by dividing the circular neighborhood into 6 sectors. More details can be found in the GMT documentation (GMT, 2021).

The map obtained from experimental data (Fig. 7a) shows that an earthquake of approximately M_L 1 is detected by a maximum of six–seven stations in a large area of the eastern

island, whereas the number of triggered stations reduces to one–two in some restricted areas, namely in the extreme areas to west and east of the southern coast and in a small area of the northern coast, respectively.

The maps shown in Figure 7b–d represent the theoretical results of the number of stations triggered by an $M_L \approx 1.0$ earthquake obtained for SNR values ranging from 3 to 5, respectively. A more complete set of maps for a wider range of SNR and number of stations' combinations is shown in Figures S2 and S3.

Figure 7 quantifies clearly what is intuitively expected, that is, that the number of triggered stations decreases when the SNR requested for declaring a trigger increases. This confirms the great importance of this parameter for determining the network performance.

The theoretical map of Figure 7d, which represents the results obtained for SNR = 5, has high coherency with that of Figure 7a, which represents the 2020 catalog data. Some minor inconsistencies may be due to several reasons, such as (1) the fact that the assumed noise level estimated from the annual average of several PSD curves (approximately 17,000 per year) does not match the noise level that actually occurs during each event; (2) the fact that, whereas the theoretical calculation includes only stations from the Cuban seismic network, the 2020 catalog was constructed using also some stations belonging to other networks in the Caribbean area; and, (3) the lack of actual earthquakes in some parts of the study area, compared with the fact that the theoretical method calculates a theoretical amplitude at each station from a uniform network of points.

In any case, our results obtained for the Cuban network confirm that our method can successfully estimate the detection capability of a seismic network from the measured noise levels at each station. Moreover, the obtained results are good enough to identify the weak elements of a seismic network and help to define some strategies for its improvement.

Conclusions

In our study, we have estimated the detection capability of the Cuban seismic network and validated our estimations with the data of the Cuban 2020 earthquake catalog. We can draw the following conclusions.

At present, with the existing technological infrastructure of the Cuban seismic network, an $M_L \approx 1.0$ earthquake can be detected by at least three stations only if it occurs in the eastern part of the country or in some restricted areas of the center or the west of the island. Any $M_L \approx 1.0$ (or larger) earthquake occurring on the Cuban territory or near to it triggers at least one station of the Cuban network. Our study suggests that $M_L \approx 2.0$ is the minimum detectable magnitude for accurately localized earthquakes (i.e., determined by at least three stations) occurring over 90% of the Cuban territory, the only exception being the westernmost extreme of the island. To reach a homogeneous capability of detection of an $M_L \approx 1.0$ earthquake (assumed as a target of minimum magnitude) over the whole Cuban territory, the network should be densified in the central and western areas of the country.

The background seismic noise is the factor that mostly affects the overall network performance, and the detection threshold worsens significantly (i.e., the minimum detected magnitude increases) with the increase of the seismic noise level. This may be due to several causes. Some of them are out of human control, such as bad atmospherical or ocean conditions. Others, as the station location and site conditions, are strictly related to a human choice, and therefore the background seismic noise can be reduced by some suitable actions, such as using posthole or borehole instruments, providing a correct thermal and electromagnetic isolation of the instruments, or ultimately moving the station to a better location. Figure S1 reports the PSD of all stations of the Cuban seismic network. At visual analysis, the following six stations should be improved for different reasons: CAIB (panel a), CAMR (panel b), CHIV (panel d), CJAG (panel e), MARV (panel h), and PILO (panel l).

Our study has been successfully validated by comparing the theoretical estimations in terms of number of triggered stations for an M_L 1.0 earthquake with those obtained for the 2020 earthquake catalog.

The applied method turns out to be a practical and effective way also for evaluating the performance of a seismic network, including how it changes in time—a feature that we have not explored in this article—and offers a wide range of automation possibilities in conjunction with some well-known seismological software such as SeisComP3 and PQLX.

The location of the Cuban island right in the middle of the Caribbean Sea can provide a strategic contribution to improve the performance of the Caribbean monitoring system, with relevant outcomes for both the alert system and the study of the seismicity on a regional scale. Not only is the Cuban territory adjacent to some relevant active structures, such as the Oriente fault system, but it also is a privileged observatory for the Haiti seismicity—an area still poorly covered by seismic stations—and in general for depicting the image of the seismicity of the whole Caribbean region. Our study suggests, on the one hand, the directions for improving the monitoring capability, and, on the other hand, it indicates the magnitude threshold that can be assumed homogeneously for the 2020 Cuban earthquake catalog.

Data and Resources

The Cuban seismic network (National Seismological Service [SSN]; www.cenais.cu; last accessed August 2021—*Rev. Fac. Ing. UCV*, June 2014, Vol. 29, no. 2, pp. 69–77. ISSN 0798-4065) is managed by the National Centre for Seismological Research (CENAIS) of the Cuban Ministry of Science, Technology and Environment (CITMA). The general SSN earthquake catalog is available for consultation at http://www.cenais.cu (last accessed February 2021). All stations are registered at the International Federation of Digital Seismograph Networks (FDSN; http://www.fdsn.org/; last accessed August 2021). The following software systems were used: SEISAN (Ottemoller and Havskov, 2014; https://www.uib.no/en/rg/geophysics/54592/software#seisan; last accessed

August 2021); Generic Mapping Tools (GMT; Wessel and Smith, 1991; Wessel *et al.*, 2013; https://www.generic-mapping-tools.org; last accessed August 2021); AWK (Aho *et al.*, 1987), with its GNU implementation GAWK (www.gnu.org/software/gawk; last accessed August 2021); PQLX (McNamara and Boaz, 2010; https://ds.iris.edu/ds/nodes/dmc/software/downloads/pqlx/2011365p4/; last accessed August 2021); and MATLAB, version 9.0.0 (R2016b), Natick, Massachusetts: The MathWorks Inc. (https://www.mathworks.com/products/matlab.html; last accessed August 2021). This article is accompanied by the supplemental material, which includes the following materials: the Cuban 2020 earthquake catalog (Data set DS01); the probability density functions calculated from the continuous recordings of seismic noise for all stations of the Cuban seismic network (Fig. S1); the estimated detection levels of the Cuban seismic network in terms of minimum detected magnitude (Fig. S2), and the number of triggered stations for an M_L 1.0 earthquake hypothetically located at each point of the study area (Fig. S3).

Declaration of Competing Interests

The authors acknowledge there are no conflicts of interest recorded.

Acknowledgments

The authors acknowledge the full collaboration of the colleagues from the Cuban National Seismological Centre during various stages of our research; they especially thank Maribel Leyva Arias and Enrique Arango for their help in extracting data from the seismic catalog and for their quick help in solving the problems derived from the selection of the data that were used in this study. This research was mainly carried out during some visiting periods of Eduardo Rafael Diez Zaldívar at Istituto Nazionale di Oceanografia e di Geofisica Sperimentale (OGS), in Italy. Those visits were partially supported by the Abdus Salam International Center for Theoretical Physics (ICTP), within the Training and Research in Italian Laboratories program (TRIL); the authors thank ICTP for the excellent support provided for arranging all the aspects of the visits. Even if not cited explicitly in the text, this study was also motivated by the need of assessing the detection performance of two local seismic networks managed by OGS for the seismic monitoring of two underground gas storages located in northern Italy at Collalto (Veneto region) and Cornegliano Laudense (Lombardia region), respectively; in this regard, the authors acknowledge that this study was partially funded by Edison Stoccaggio S.p.A., the storage concession holder, under Contract Number 1500118977 CO established between Edison Stoccaggio S.p.A. and OGS on 11 December 2019, and by Ital Gas Storage S.p.A., under a research contract established among Ital Gas Storage S.p.A., OGS, and Consiglio Nazionale delle Ricerche, Istituto per il Rilevamento Elettromagnetico dell'Ambiente (CNR-IREA), Napoli, Italy on 16 February 2018, respectively. Finally, the authors would like to thank the two reviewers (Thomas Braun and an anonymous reviewer) and Editor-in-Chief Allison Bent for their thorough review and clear and constructive suggestions, which helped them improve this article considerably.

References

Aho, A. V., B. W. Kernighan, and P. J. Weinberger (1987). *The AWK Programming Language*, Addison-Wesley Longman Publishing Co., Inc., Boston, MA, United States.

Aki, K., and P. G. Richards (1980). *Quantitative Seismology, Theory and Methods. Volume I: 557 pp., 169 Illustrations. Volume II: 373 pp., 116 Illustrations*, ISBN 0-7167-1058-7 (Vol. I), 0-7167-1059-5 (Vol. II), Freeman, San Francisco, California.

Álvarez, L. (2000). *Sismicidad de Cuba y estructura de la corteza en el Caribe*, ISBN 959-02-0242-X, Editorial Academia, La Habana, Cuba.

Álvarez, J. L., and V. I. Bune (1977). Estimación de la peligrosidad sísmica de la región suroriental de Cuba, *Fizika Zemli*, no. 10, 54–67 (in Russian).

Álvarez, L., T. Chuy, and M. Cotilla (1991). Peligrosidad sísmica de Cuba. Una aproximación a la regionalización sísmica del territorio nacional, *Revista Geofísica del Instituto Panamericano de Geografía e Historia*, no. 35, 125–150 (in Spanish).

Álvarez, L., T. Chuy, J. García, B. Moreno, H. Álvarez, M. Blanco, O. Expósito, O. González, and A. I. Fernández (1999). An earthquake catalogue of Cuba and neighbouring areas, *ICTP Internal Rept. ic/ir/99/1*, Miramare, Trieste, Italy, 60 pp.

Arango, E. D. A. (2009). Análisis geodinámico y sismotectónico del extremo oriental de Cuba, *Acta GGM Debrecina* **4,** 43–52 (in Spanish).

Arango, E. D. A. (2021). Sismicidad Registrada en el territorio nacional y estado de la red de estaciones del servicio sismológico nacional, *Vicedirección Técnica, Archivos de Centro Nacional de Investigaciones Sismológicas, Ministerio de Ciencia, Tecnología y Medio Ambiente, 2020* (in Spanish).

Bormann, P., and E. A. Bergman (2002). The new IASPEI manual of seismological observatory practice (NMSOP), *Seismol. Res. Lett.* **71,** no. 5, 510–518.

Brune, J. N. (1970). Tectonic stress and spectra of seismic shear waves from earthquake, *J. Geophys. Res.* **75,** 4997–5009.

Calais, E., and M. Lépinay (1989). Géométrie et régime tectonique le long d une limite de plaques en coulissage: la frontiére nord-Caraïbe de Cuba á Hispaniola Grandes Antilles, *Géodynamique. C R. Acad. Sci. Paris, t.* **308,** 131–135 (in French).

Calais, E., and M. Lépinay (1993). Semiquantitative modeling of strain and kinematics along the Caribbean/North America strike-slip plate boundary zone, *J. Geophys. Res. Atmos.* **98,** 8293–8308.

CENAIS (2020). Catálogo de terremotos (extracción parcial del año 2020 del catalogo general de terremotos), *Fondos del CENAIS* (in Spanish).

Chuy, T. (1999). Macrosísmica de Cuba y su aplicación en los estimados de peligrosidad y microzonación Sísmica, *Tesis en opción al Grado de Doctor en Ciencias Geofísicas, Fondos del MES y CENAIS*, 150 pp. (in Spanish).

Clinton, J., G. Cua, V. Huérfano, C. von Hillebrandt-Andrade, and J. Martinez Cruzado (2006). The current state of seismic monitoring in Puerto Rico, *Seismol. Res. Lett.* **77,** 532–543.

D'Alessandro, A., D. Luzio, G. D'Anna, and G. Mangano (2011). Seismic network evaluation through simulation: An application to the Italian National Seismic Network, *Bull. Seismol. Soc. Am.* **101,** 1213–1232.

De Zeeuw-van Dalfsen, E., and R. Sleeman (2018). A permanent, real-time monitoring network for the volcanoes mount scenery and the Quill in the Caribbean Netherlands, *Geosciences* **8,** no. 9, doi: 10.3390/geosciences8090320.

DeMets, C. (1990). Earthquake slip vectors and estimates of present-day plate motions, *J. Geophys. Res.* **98,** no. B4, 6703–6714.

Deng, J., and L. Sykes (1995). Determination of Euler polo for contemporary relative motion of Caribbean and North American plates using slip vectors of interpolate earthquakes, *Tectonics* **14,** no 1, 39–53.

Diez Zaldívar, E. (1999). Cuban National Seismo-Telemetric Network, *Abdus Salam Internacional Centre for Theoretical Physics (ICTP)*, Preprint 1999038.

Diez Zaldívar, E. R., M. C. Mustelier, C. M. Moracén, R. P. Cláres, V. Poveda Brossard, Z. Yinxing, C. Yang, and W. Fengxia (2014). Modernización de la red sísmica cubana. Instalación, calibración y puesta a punto, *Revista de la Facultad de Ingeniería Universidad Central de Venezuela* **29,** no. 2, 69–78 (in Spanish).

Franceschina, G., P. Aaugliera, S. Lovati, and M. Massa (2015). Surface seismic monitoring of a natural gas storage reservoir in the Po Plain (northern Italy), *Boll. Geof. Teor. Appl.* **56,** no. 4, 489–504, doi: 10.4430/bgta0165.

Gestermann, N., T. Plenefisch, T. Kraft, and M. Herrmann (2016). Seismic network detection capability within the natural gas fields in northern Germany, *ESC General Assembly 2016*, Trieste (Italy), ESC2016-511, Poster.

GMT (2021). The Generic Mapping Tools documentation, *The GMT Team*, available at https://docs.generic-mapping-tools.org/latest/# (last accessed February 2021).

Gonzales, O. F., and E. D. Arango (1996). *Boletín Sismológico Cubano, Red de estaciones e investigaciones sismológicas en Cuba*, ISBN 959-02-0244-6, Editorial Academia, La Habana, Cuba, 7–17.

Greig, W., and N. Ackerley (2014). Microseismic network performance estimation: Comparing predictions to an earthquake catalogue, *EGU General Assembly Conference 2014, Geophys. Res. Abstracts*, Vol. 16, EGU2014-6361.

Helmholtz-Centre Potsdam—GFZ German Research Centre for Geosciences and gempa GmbH (2008). The SeisComP seismological software package, *GFZ Data Services*, doi: 10.5880/GFZ.2.4.2020.003.

Heubeck, C., and P. Mann (1991). Geologic evaluation of plate kinematic models for the North American-Caribbean plate boundary zone, *Tectonophysis* **191,** 1–26.

IRIS (2017). Software downloads—PQLX, Incorporated Research Institutions for Seismology, available at https://ds.iris.edu/ds/nodes/dmc/software/downloads/pqlx/ (last accessed February 2022).

IRIS (2022). miniSEED, Incorporated Research Institutions for Seismology, available at https://ds.iris.edu/ds/nodes/dmc/data/formats/miniseed/ (last accessed February 2022).

Lundgren, P. R., and R. M. Russo (1996). Finite element modelling of crustal deformation in the North America-Caribbean plate boundary zone, *J. Geophys. Res.* **101,** no. B5, 11,317–11,327.

Mann, P. (1999). Caribbean sedimentary basins: Classification and tectonic setting, in *Sedimentary Basins of the World, Caribbean Basins*, P. Mann (Editor), Elsevier, Amsterdam, Netherlands, 3–31.

Mann, P., E. Calais, and V. Huérfano (2004). Earthquake shakes big bend region of North America Caribbean boundary zone, *EOS Trans. AGU* **85,** 24 pp.

Mann, P., F. Taylor, R. Edwards, and T.-L. Ku (1995). Actively evolving microplate formation by oblique collision and side-ways motion along strike-slip faults: An example from the northeastern Caribbean plate margin, *Tectonophysics* **246,** 1–69.

Marzorati, S., and M. Cattaneo (2016). Stima automatica della magnitudo minima rilevabile dalla rete sismica ReSIICO—Automatic magnitude detection of the seismic network ReSIICO, *Quaderni di Geofisica 2016, Istituto Nazionale di Geofisica e Vulcanologia (INGV)*, 21 pp. (in Italian).

McNamara, D. E., and R. I. Boaz (2005). Seismic noise analysis system using power spectral density probability density functions: A stand-alone software package, *U.S. Geol. Surv. Open-File Rept. 2005-1438*, U.S. Department of the Interior, U.S. Geological Survey.

McNamara, D. E., and R. I. Boaz (2010). PQLX: A seismic data quality control system description, applications, and user's manual, *U.S. Geol. Surv. Open-File Rept. 2010-1292*, doi: 10.3133/ofr20101292.

McNamara, D. E., C. Von Hillebrandt-Andrade, J. M. Saurel, V. Huerfano, and L. Lynch (2016). Quantifying 10 years of improved earthquake monitoring performance in the Caribbean region, *Seismol. Res. Lett.* **87,** no. 1, doi: 10.1785/0220150095.

Moreno, B. (2002a). The new Cuban seismograph network, *Seismol. Res. Lett.* **73,** 504–517.

Moreno, B. (2002b). New magnitude scales and attenuation relation for eastern Cuba, *Ph.D. Thesis*. Crustal structure and seismicity of Cuba and web-based applications for earthquake analysis, University of Bergen, Norway.

Moreno, B., M. Grandison, and K. Atakan (2002). Crustal velocity model along the southern Cuba margin. Implications for the tectonic regime at an active plate boundary, *Geophys. J. Int.* **151,** 632–645.

Nanjo, K. Z., D. Schorlemmer, J. Woessner, S. Wiemer, and D. Giardini (2010). Earthquake detection capability of the Swiss seismic network, *Geophys. J. Int.* **181,** no. 3, 1713–1724.

Ottemoller, V., and J. Havskov (2014). Seisan earthquake analysis software for Windows, *Solaris, Linux and Macosx, 2014*.

Peterson, J. (1993). Observation and modelling of seismic background noise, *U.S. Geol. Surv. Open-File Rept. 93-322*, 95 pp.

Petersen, G. M., S. Cesca, M. Kriegerowski, and , and the AlpArray Working Group (2019). Automated quality control for large seismic networks: Implementation and application to the alparray seismic network, *Seismol. Res. Lett.* **90,** no. 3, 1177–1190, doi: 10.1785/0220180342

Poveda Brossard, V., and E. R. Diez Zaldívar (2022). Ambient seismic noise in Cuba: analysis of broadband seismic stations in the Cuban seismic network, *DYNA* **89,** no. 220, 145–153, doi: 10.15446/dyna.v89n220.96966.

Raymer, D. G., and H. D. Leslie (2011). Microseismic network design - estimating event detection. 73rd EAGE Conference and Exhibition 2011 incorporating SPE EUROPEC 2011: Unconventional Resources and the Role of Technology, *EAGE* **2011,** no. 1, 595–599.

Rosencrantz, E., and P. Mann (1991). SeaMARC II mapping of transform faults in the Cayman trough, Caribbean Sea, *Geology* **19,** no. 7, 690–693.

Schorlemmer, D., and J. Woessner (2008). Probability of detecting an earthquake, *Bull. Seismol. Soc. Am.* **98,** no. 5, 2103–2217.

Serrano, M., and L. Álvarez (1983). Desarrollo de la sismología instrumental en Cuba, *Investigaciones Sismológicas en Cuba*, no. 4, 5–20 (in Spanish).

Wessel, P., and W. Smith (1991). Free software helps map and display data, *EOS Trans. AGU* **72,** 441–461.

Wessel, P., W. H. F. Smith, R. Scharroo, J. F. Luis, and F. Wobbe (2013). Generic mapping tools: Improved version released, *EOS Trans. AGU* **94,** 409–410, doi: 10.1002/2013EO450001.

Zivčić, M., and J. Ravnik (2002). Detectability and earthquake location accuracy modeling of seismic networks, IS 7.4, in *New Manual of Seismological Observatory PracNce*,P. Bormann (Editor), Vol. 1, GeoForschungsZentrum, Potsdam, Germany.

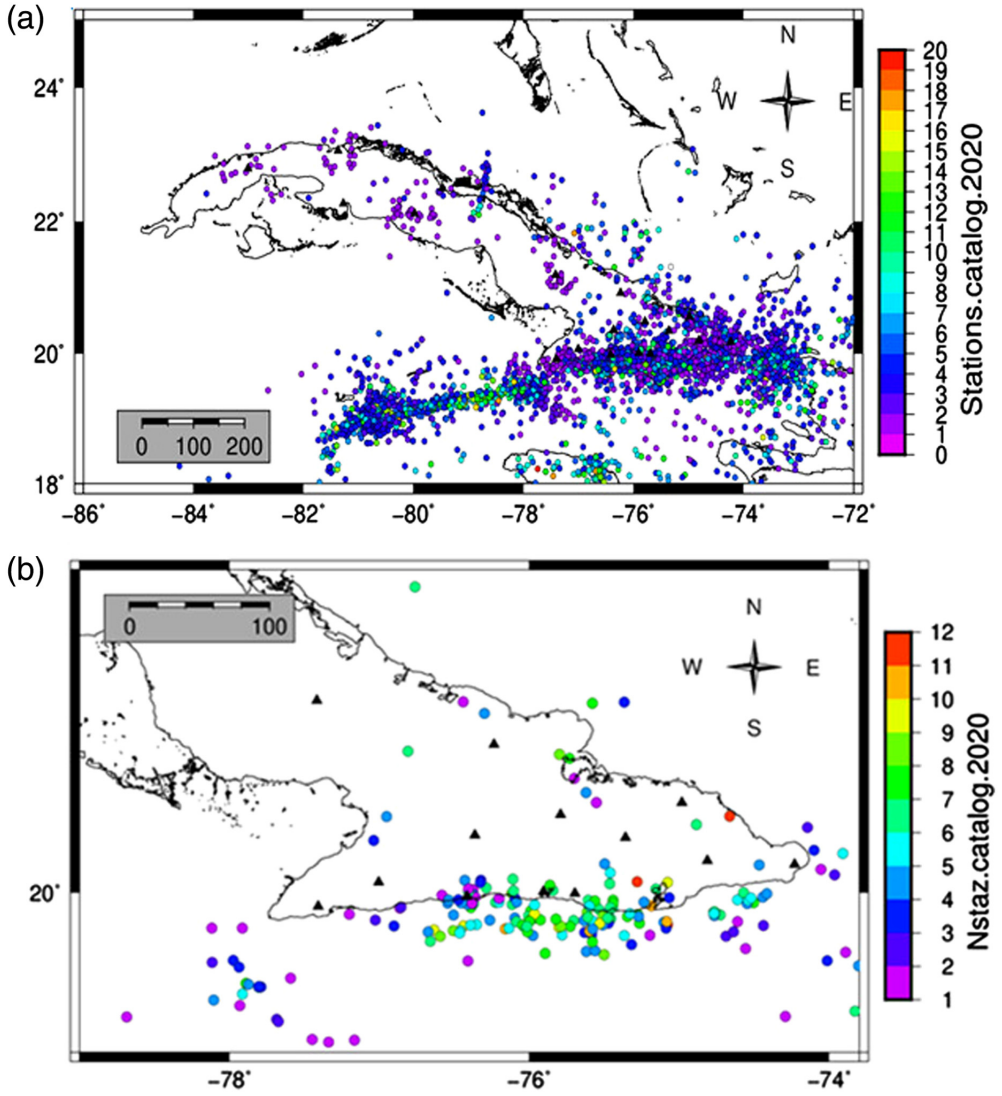

Figure A1. Seismicity of the year 2020 in Cuba and surrounding areas, extracted from the National Centre for Seismological Research catalog and corresponding to the data of the 2020 earthquake catalog delivered as Data set DS01. (a) All earthquakes recorded in 2020. (b) Events with $0.9 \le M_L \le 1.1$ localized in the eastern part of Cuba. For each event, the color corresponds to the number of the triggered stations. Black triangles: location of the seismic stations. The color version of this figure is available only in the electronic edition.

Appendix

We have extracted from the earthquake catalog Cuban National Seismological Centre a selection corresponding to the earthquakes that occurred in the year 2020. This catalog has been used for validating the results of the theoretical estimations of the detection capability of the Cuban seismic network. The 2020 earthquake catalog reports all earthquakes detected and localized in the region surrounding the Cuba island. The catalog uses data not only of the Cuban seismic network but also of other stations of the Caribbean region, and it also reports recognized by manual inspection, in some cases triggered by one station.

Figure A1 shows the maps of the 2020 catalog for the whole Cuban territory (panel a) and of the events with $0.9 \le M_L \le 1.1$ localized in the eastern part of the island, respectively. (panels a and b, respectively). For each event, the color corresponds to the number of the triggered stations.

The Cuban 2020 earthquake catalog is delivered as the supplemental material to this article as Data set DS01.

Manuscript received 12 January 2022
Published online 2 June 2022